NMR Backbone Assignment of a Protein Kinase Catalytic Domain by a Combination of Several Approaches: Application to the Catalytic Subunit of cAMP-Dependent Protein Kinase

Thomas Langer,* Martin Vogtherr, Bettina Elshorst, Marco Betz, Ulrich Schieborr, Krishna Saxena, and Harald Schwalbe*[a]

Protein phosphorylation is one of the most important mechanisms used for intracellular regulation in eukaryotic cells. Currently, one of the best-characterized protein kinases is the catalytic subunit of cAMP-dependent protein kinase or protein kinase A (PKA). PKA has the typical bilobular structure of kinases, with the active site consisting of a cleft between the two structural lobes. For full kinase activity, the catalytic subunit has to be phosphorylated. The catalytic subunit of PKA has two main phosphorylation sites: Thr197 and Ser338. Binding of ATP or inhibitors to the ATP site induces large structural changes. Here we describe the partial backbone assignment of the PKA catalytic domain by NMR spectroscopy, which represents the first NMR assignment of any protein kinase catalytic domain. Backbone resonance assignment for the 42 kDa protein was accomplished by an approach employing 1) triply (^{2}H,^{13}C,^{15}N) labeled protein and classical NMR assignment experiments, 2) back-calculation of chemical shifts from known X-ray structures, 3) use of paramagnetic adenosine derivatives as spin-labels, and 4) selective amino acid labeling. Interpretation of chemical-shift perturbations allowed mapping of the interaction surface with the protein kinase inhibitor H7. Furthermore, structural conformational changes were observed by comparison of backbone amide shifts obtained by 2D ^{1}H,^{15}N TROSY of an inactive Thr197Ala mutant with the wild-type enzyme.

Introduction

Protein phosphorylation and dephosphorylation are critical integral parts of signal transduction events enabling cells to respond to external stimuli. This is achieved by protein kinases catalyzing the transfer of the γ-phosphate from ATP to a target protein and thereby altering the activation state of the target protein. The reverse reaction, dephosphorylation, is accomplished by various protein phosphatases. Many kinases are themselves also phosphorylated, and phosphorylation often leads to activation or "switching on" of the kinases. Kinetic activity is reduced by dephosphorylation or "switching off". Within the human genome, 518 putative protein kinase genes have been identified.[1] Due to their importance in intracellular signaling, deregulation of protein kinases can cause various diseases.[2,3] All known protein kinase catalytic domains share the same bilobular tertiary structure, with the active site located in a cleft between the two lobes. The smaller N-terminal lobe containing the ATP-binding site consists mainly of β-sheets, while the C-terminal lobe comprising the protein-substrate-recognition elements is predominantly α-helical.

The PKA-holoenzyme is made up of two regulatory subunits and two catalytic subunits. Upon binding of cAMP to the regulatory subunits, the PKA catalytic subunits are released (reviewed in[5]). For full catalytic activity, the catalytic subunit has to be phosphorylated. Indeed, the phosphorylation of residues Thr197 and Ser338, situated in the catalytic subunit, is quite stable even in the presence of phosphatases, and these phosphorylation sites have also been termed "stable" or "silent".[6] In eukaryotic cells, PKA catalytic activity is controlled by association of the phosphorylated catalytic subunit with the regulatory subunits. The PKA catalytic subunit can also be expressed recombinantly in *E. coli*; the protein is phosphorylated due to its autocatalytic activity.[7] Furthermore, Ser10 and Ser139 are also phosphorylated in the recombinant protein. Isoforms containing two, three, and four phosphate groups can be discriminated, and phosphorylation on Ser139 seems to occur only in *E. coli*.[8,9] No physiological functions have been reported for the two phosphorylation sites S10 and S139. Thr197 lies in the activation loop and phosphorylation is required for ATP binding. Ser338 is located in the hydrophobic motif at the C terminus.

More than 100 physiological targets of PKA have so far been described.[10] Due to this broad substrate spectrum and its multiple functions, PKA is currently not considered to be a pharmaceutical target. However, because of the high degree of structural and functional conservation within the protein

[a] *Dr. T. Langer, Dr. M. Vogtherr, Dr. B. Elshorst, Dr. M. Betz, Dr. U. Schieborr, Dr. K. Saxena, Prof. Dr. H. Schwalbe*
Johann Wolfgang Goethe-Universität Frankfurt
Institute for Organic Chemistry and Chemical Biology
Center for Biomolecular Magnetic Resonance
Marie Curie Straße 11, 60439 Frankfurt am Main (Germany)
Fax: (+49) 69-798-29515
E-mail: t.langer@nmr.uni-frankfurt.de
schwalbe@nmr.uni-frankfurt.de

  DOI: 10.1002/cbic.200400129

kinase family, and since large amounts of recombinant and active catalytic subunit PKA can easily be obtained, this protein kinase has become a model kinase for all other kinases.[11,12] Numerous X-ray structures of free PKA and of inhibitor- and substrate-bound complexes are available (reviewed in[4]). However, the structure of the non-phosphorylated and hence inactive PKA is unknown. The conserved PKA catalytic subunit core encompasses amino acids 40–300.[13] Unique features of the PKA catalytic subunit are the A-helix (amino acids 16–31) bearing an *N*-myristylation motif, and a 50-residue extension at the C terminus with a FTEF sequence. This amino acid stretch folds back to the N-terminal lobe where the sidechains of the phenylalanines are bound in a hydrophobic cleft.[4]

Protein kinases are rather flexible molecules. Conformation and dynamic behavior depend on the activation status and on the binding of substrates.[14] The available X-ray structures have provided important snapshots of the protein in different states;[15–17] however, these structures do not provide a detailed view of the underlying dynamic processes. Spectroscopic techniques are therefore an ideal complement to the available structural data. In particular, NMR allows monitoring of a wide range of motional processes by relaxation analysis, and of global large-scale motions by evaluation of residual dipolar couplings. Up to now, no assignment of the NMR signals of any protein kinase catalytic domain is publically available. Recent developments have made proteins of this size amenable to modern NMR methods; however, assignment of such a protein is clearly non-standard. Here we report on the NMR resonance assignment of 70% of all resolved NMR peaks; this corresponds to 56% of the number of amino acids, by a combination of several approaches that should be generally applicable to other protein kinases.

Results

Composition of the NMR sample

All NMR experiments require homogeneous, side-chain-deuterated and backbone-protonated proteins. Side-chain deuteration, as judged from the ^{1}H NMR, is nearly complete. Since the cells were grown in aqueous medium, there are no intensity losses due to incomplete back-exchange of hydrogen-bonded protons.

The PKA catalytic subunit can be phosphorylated at four different sites when expressed in *E. coli*.[7–9] The phosphorylation statuses of the protein samples were analyzed by ^{31}P NMR, and four ^{31}P resonances were observed (data not shown). Our results are consistent with the findings described by Seifert et al.[9]

Extent of assignment

The recombinant expressed PKA consists of 353 amino acids, eight of which are prolines. The spectra gave 274 backbone amide peaks in total, and 191 of these amide backbone resonances were assigned; this represents 70% of the total amount of resolved peaks. The extent of assignment corresponds to 55%, based on the total number of amino acids. Figure 1 shows an annotated TROSY spectrum and a mapping of assigned residues onto the structure and the sequence. Assigned regions include the N- and C-terminal sequences, most of the N lobe, including the glycine-rich loop, and most solvent-exposed residues of the C lobe. Assignments for the buried helices in the interior of the C lobe are missing. Through the use of uniform ^{2}H, ^{13}C, and ^{15}N labeling and the TROSY scheme, it is possible to achieve correlations even for large proteins.[18,19] This approach is sufficient for complete assignment of the rather flexible N and C termini of PKA. In the more rigid parts of the protein, however, many expected correlations were missing, and this resulted in incomplete NMR data sets. Furthermore, the number of possible assignments increases with the protein's size. This means that only relatively short stretches can be correlated and are difficult to "match" on the sequence.

The chemical shift matching strategy

To circumvent the "matching" problem, we employed a novel chemical shift prediction approach. Briefly, chemical shifts for backbone and Cβ are predicted from a known structure.[20] Whereas back-calculation of chemical shifts has been continuously refined over the years, its use for assignments has not been exploited so far. The reason is that for any one particular shift the error is too large, and the situation is not much better for two correlated shifts (e.g., a cross-peak in a TROSY spectrum). However, experimental data for a correlated stretch of amino acids provide enough information for a matching strategy. These empirical data are compared with predicted shifts for any possible location. At the correct location A, the agreement between the two, as expressed by a target function rmsd(*A*), becomes optimal.

Evidently, this method should be very useful in the automated assignment of proteins with known X-ray structures and with incomplete correlation data. Another benefit is the possibility to identify "wrong" correlations, since these lead inevitably to high rmsd values. We are currently exploring the limits of this approach on a broader basis of protein structures. This approach will be published in detail elsewhere.

Use of spin-labels

PKA possesses a well-characterized binding site for ATP. ATP binding induces large-scale motions of the protein.[4] Therefore, the magnitude of chemical-shift perturbations induced by ATP binding is not directly linked with proximity to the ATP binding site. In contrast, use of a paramagnetic spin-label such as spin-labeled adenosine (Scheme 1, leading to a pure distance-dependent line broadening or disappearance of signals, was the method of choice for unambiguous localization of amino acids near the ATP binding site (data not shown). Since no X-ray structure is available for the complex of PKA with spin-labeled adenosine, there is some uncertainty concerning the position of the radical center. The coordinates of the ATP β-phosphate in the PKA·ATP complex were used to approximate the posi-

Figure 1. *A) Annotated 800 MHz ^{13}C-decoupled TROSY spectrum of PKA at pH 6.0. B) Mapping of assigned amino acids on the PKA tertiary structure (pdb code 1ATP). Assigned amino acids are blue. The position of ATP in the X-ray structure is indicated. C) Mapping of assigned amino acids on the primary sequence of the construct in use. Assigned residues appear hatched. The Hanks and Hunter designation of conserved protein kinase regions appears below the sequence.[13] Phosphorylation sites are marked with asterisks.*

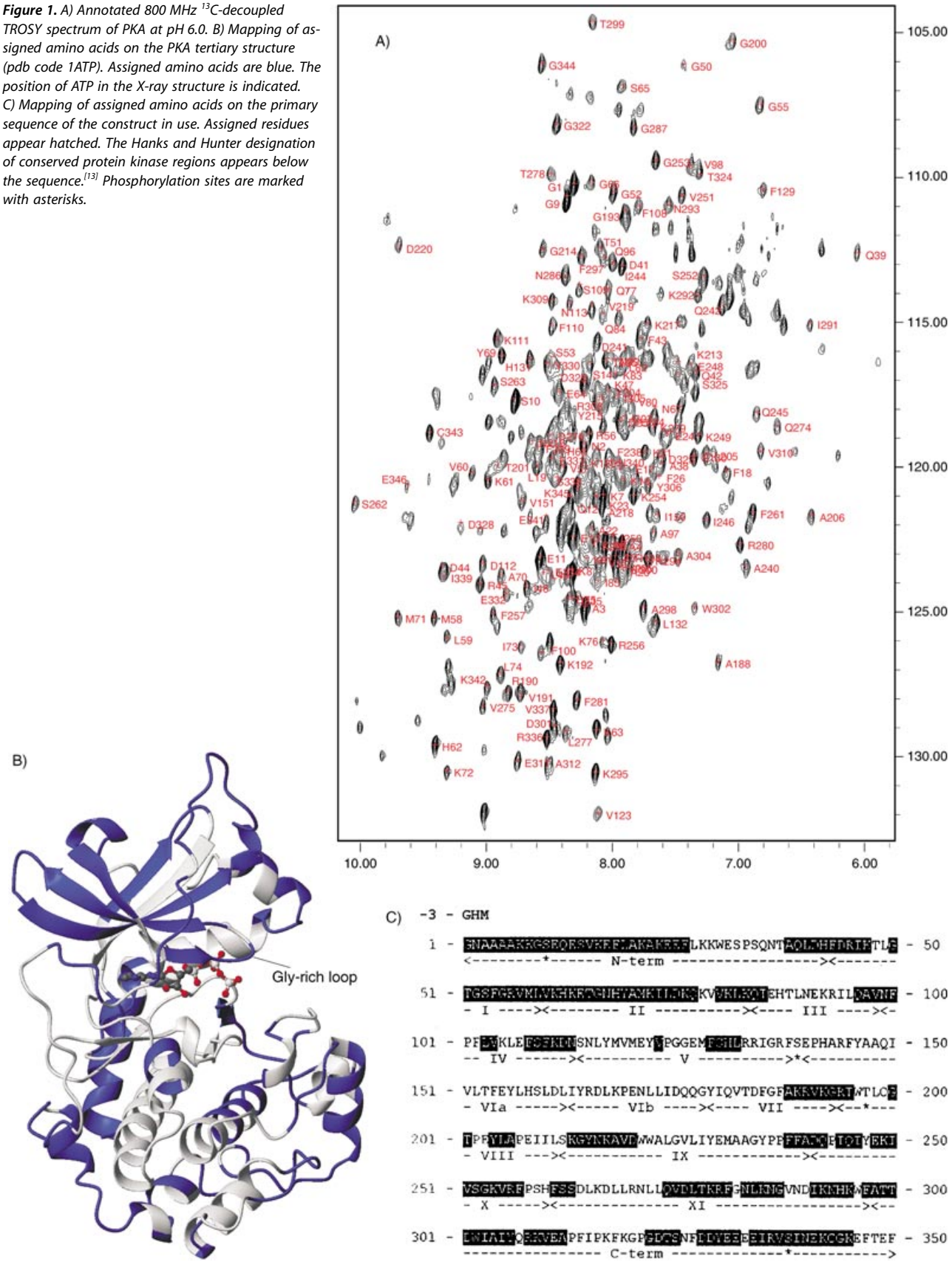

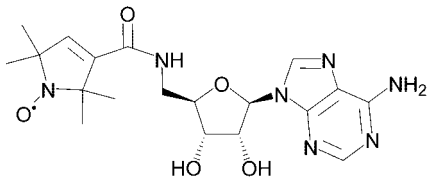

Scheme 1. *Structure of the spin-labeled adenosine (1-oxyl-2,2,5,5,-tetramethyl-pyrroline-3-carboxylate (5-aminoadenosine)-amide).*

tion of the radical center. Peaks within a radius of 20 Å around the adenosine-binding site are then affected.

PKA binds ATP·M^{2+} (M = Mg, Mn). Small amounts of Mn^{2+} are expected to induce line-broadenings arising from the structurally well-defined coordinates of the metal ion. In fact, observed line-broadening effects were dispersed over the whole protein, presumably due to unspecific binding of Mn^{2+} to negatively charged surface residues.

Selectively labeled samples

A previous study reported selective labeling of the cAbl kinase catalytic domain, which can be expressed only in insect cells, for NMR purposes.[21] Uniform labeling by expression in *E. coli* is straightforward, but the selective labeling of specific amino acids is nevertheless a very helpful approach to alleviate spectral overlap or to distinguish between two possible assignments, for example. For our purposes, PKA selectively labeled with six different ^{15}N-labeled amino acids (Phe, Tyr, Leu, Asp, Ile, Val) was used. The only observed scrambling reaction was the conversion of Asp to Asn. In that case, Asp peaks were found in the TROSY spectrum together with peaks from Asn. As an example, Figure 2 shows the annotated subspectrum of PKA selectively labeled with ^{15}N-Val.

An even higher specificity for selected sites can be achieved with ^{13}C,^{15}N double labeling and filtering by a 2D HNCO.[22] In a published version using ^{13}C,^{15}N Val only Val–Val sequences have been identified. As an extension of this approach, we used 1–^{13}C Tyr and ^{15}N Val doubly selectively labeled PKA to identify the only Tyr–Val sequence in the protein, Tyr122–Val123, which is located in the hinge region. As expected, only one peak in the 2D HNCO spectrum appeared (data not shown). This enabled us to identify the Val123 TROSY peak, which has no interresidual correlations in the 3D spectra.

Combined use of spin-labels and selectively labeled samples

The combination of selective labeling with a spin-label allows quantification of the amount of line-broadening, which is otherwise difficult due to overlapping lines. This approach leads to a more detailed picture of the distance between a given amide group and the spin-label.

Figure 3a shows a plot of relative intensities of all assigned Val signals versus their distance from the spin-label. This is schematically depicted in Figure 3b. A clear distinction between affected and unaffected peaks, dependent on the distance as expected from the r^{-6} relationship, was found. Obviously, peaks with <18 Å distance from the spin-label were affected. Val15 and Val251 are outliers. Val15, which is safely assigned on the basis of interresidual correlations, is strongly affected although it is far away from the ATP binding site. Consistently, most residues in the N-terminal helix are shifted after addition of (non-spin-labeled) adenosine. This behavior cannot be explained by available coordinates, although the non-myristylated N-terminus of PKA is highly flexible and might also adopt conformations closer to the ATP binding site. Another explanation would be to assume weak binding of adenosine to the N terminus.

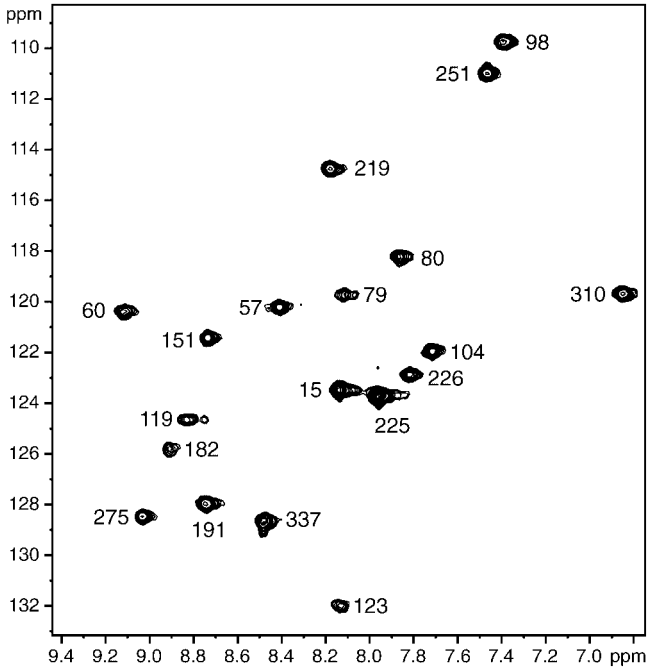

Figure 2. *Annotated TROSY spectrum of PKA selectively labeled with ^{15}N Val; 19 out of the total of 20 valine moieties gave strong peak intensities in the spectrum and could be assigned.*

With this approach, it was possible to detect and assign 19 out of the total of 20 valine residues. These experiments even enable the assignment of single valine residues that would otherwise have been difficult to assign because of weak interresidual correlations.

Mapping of a specific kinase inhibitor

Chemical shift perturbations caused by binding of the protein kinase inhibitor H7 were used to map the interaction surfaces between this compound and the protein, thereby defining the binding site, which had been previously characterized by X-ray crystallography.[23] The result is depicted in Figure 4. The main chemical shift perturbations occur in the vicinity of the crystallographically determined position of the ligand.

Mutant PKA proteins

Phosphorylation of Thr197 is required for ATP binding and hence activity. As reported earlier, the Ser338 phosphorylation

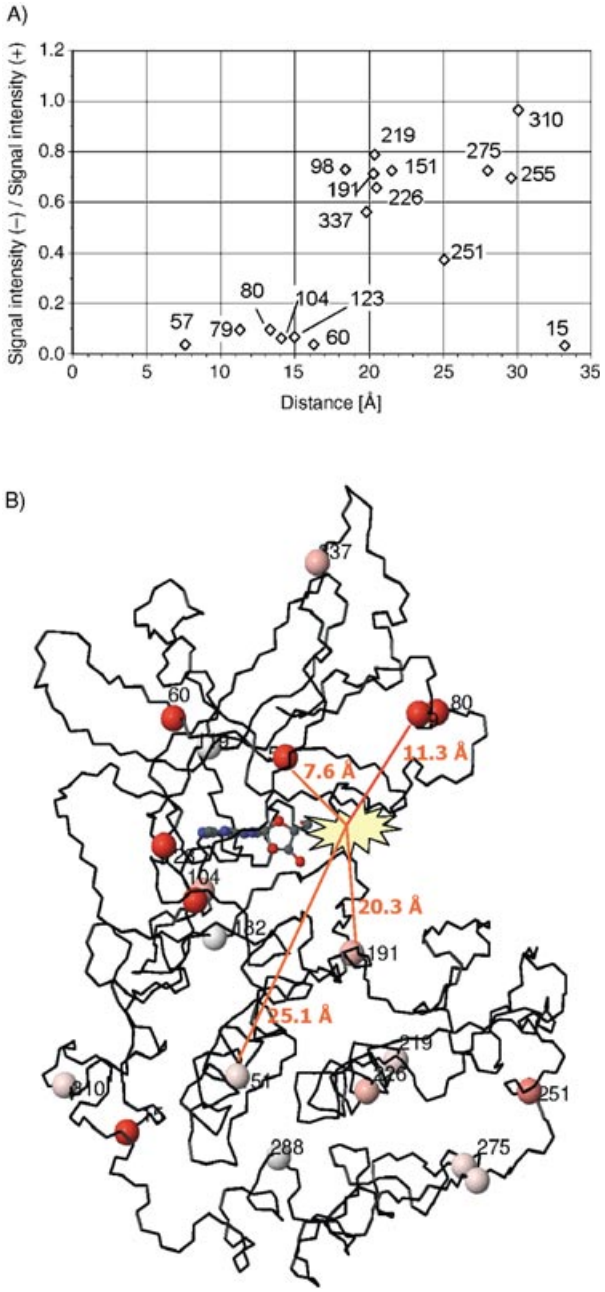

Figure 3. *A) Peak attenuation of TROSY peaks from PKA selectively labeled with ^{15}N Val upon addition of spin-labeled adenosine (0.5 mM protein, 1 mM spin-labeled adenosine). Peaks are labeled with their assignment. The ratio of the signal intensity without the spin-label (−) to the signal intensity with the spin-label added (+) was plotted against the distance from the assumed paramagnetic center to the corresponding valine residue. The plot represents the expected r^{-6} relationship between attenuation and distance, except for Val15 in the flexible N-terminus. B) Mapping of assigned valines that are affected upon addition of the spin-label. The position of the adenosine moiety from ATP as in the X-ray structure is indicated. The spin-label paramagnetic center, depicted as the yellow star, is assumed to be located in the place occupied by the β-phosphate of ATP. Some distances from the paramagnetic center to various valine residues are indicated. The different color intensities display the impact of the spin-label on the line-broadening. Signal intensities from valines 182 and 288 are not affected by the spin-label.*

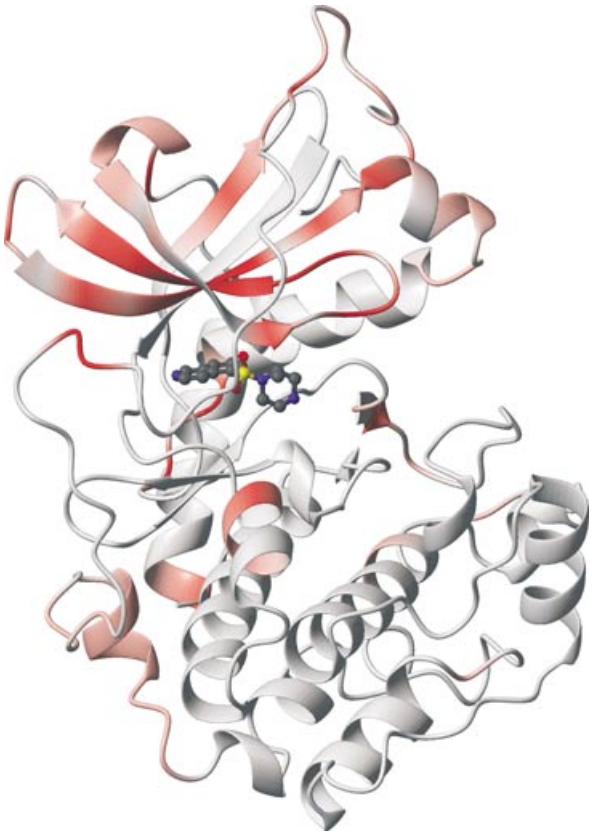

Figure 4. *Mapping of the interaction between H7 and PKA. Amino acids which show chemical shifts upon addition of H7 are assigned in red, depending on the strength of peak shift. Most of the shifted peaks are located in the ATP-binding site.*

enhances protein stability.[7] Figure 5 shows the positions of Thr197 and Ser338 within PKA. The phosphate groups of both the Thr197 and the Ser338 residues have various contacts to other side chains. An intriguing question is whether replacement of Thr197 or Ser388 by Ala would have structural consequences. Both PKA mutants, Thr197Ala and Ser338Ala, could be expressed in *E. coli* in amounts comparable to that of the wild-type protein. Both mutants are less stable than the wild-type enzyme, a feature also described in an earlier report.[7] The instability of the proteins increases, the more highly concentrated the protein is. This led to quality losses in the corresponding TROSY spectra relative to that of the wild type. At lower protein concentrations (up to ca. 2 mg mL^{-1}), however, these proteins were stable for weeks at 4 °C. A double mutant Thr197Ala/Ser338Ala could also be expressed, but this mutant turned out to be highly unstable and tended toward aggregation (data not shown). Catalytic activity was checked with the aid of a luminescent kinase assay. The K_I value of H7 was calculated to be 3.9 ± 1.1 μM for the wild type and 4.9 ± 1.1 μM for the Ser338Ala mutant protein (Figure 6). These results are in good agreement with previously reported values for H7 and PKA.[11,24] The Thr197Ala PKA mutant enzyme did not show any catalytic activity.

In order to investigate the folding of the Thr197Ala and Ser338Ala mutants, proteins were labeled with ^{15}N, and a

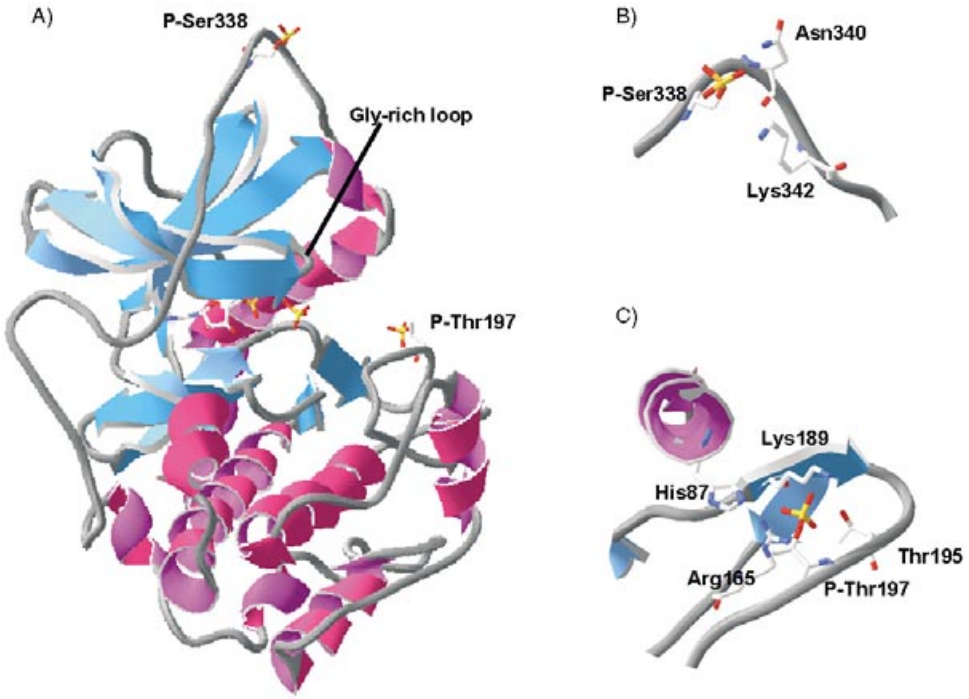

Figure 5. *Structure of the PKA catalytic subunit. The structure is drawn from pdf-file 1ATP with Swiss pdb-Viewer. A) Overall structure. The positions of phosphorylated Thr197 in the activation loop and Ser338 in the hydrophobic C terminus are indicated. B) P-Ser338 makes contacts to side chains of Asn340 and Lys342. C) P-Thr197 is in contact with the side-chains of His87, Arg165, Lys189, and Thr195.*

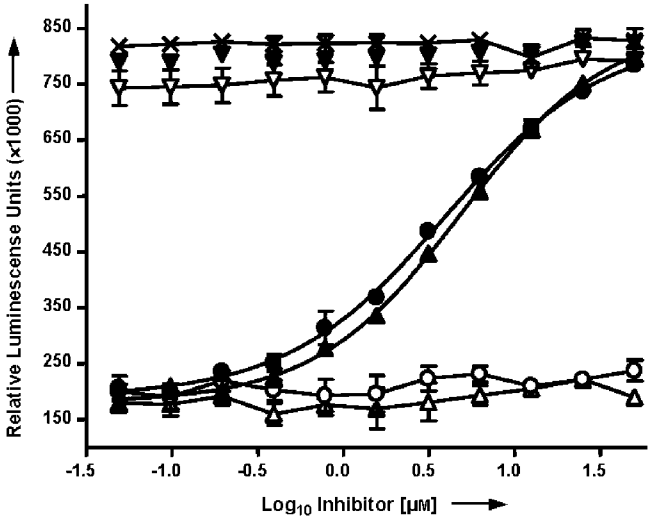

Figure 6. *Enzymatic activity of wild-type PKA compared with the PKA Thr197Ala and PKA Ser338Ala mutants. Error bars represents the standard error of the mean (SEM). × No kinase added, ○ PKA wild type (no inhibitor), △ Ser338Ala (no inhibitor), ▽ Thr197Ala (no inhibitor), ● PKA wild-type + H7, ▲ Ser338Ala + H7, ▼ Thr197Ala + H7. For experimental details see Experimental Section.*

TROSY-NMR spectrum was recorded for each protein (Figure 7). The peak pattern of the Ser338Ala mutant neatly matches the pattern of the wild-type enzyme, whereas the Thr197Ala protein yielded a different peak pattern. These results are indicative of a different conformation in at least some regions of the Thr197Als mutant in relation both to the wild-type and the Ser338Ala mutant protein.

Discussion

Experimental approach: A combination of classical schemes is successful

NMR spectroscopy of large proteins is a challenging task and the search for novel experimental schemes is still ongoing. In our case the need for novel experiments is stressed by the fact that only 80% of the backbone amide signals led to resolved peaks, whereas 20% of the expected amide signals remain undetectable even in TROSY-based triple resonance spectra.

Here we have shown that good results can also be achieved by a combination of several "classical" approaches: 1) uniform triple $^{2}H,^{13}C,^{15}N$-labeling in conjunction with classical 3D experiments and TROSY, 2) back-calculation of chemical shifts from known X-ray structures, 3) use of paramagnetic adenosine derivatives as spin-labels, and 4) selective amino acid labeling. There is no need to discuss the use of the two last schemes, which have been put to good use in biomolecular NMR for a long time. Instead, we want to stress the importance of the chemical shift matching scheme.

Protein kinase catalytic domains become accessible to NMR

Despite the variety and importance of kinases, there are at present no assignment data of a protein kinase catalytic domain available. Published NMR studies on kinase catalytic domains are restricted to a subset of NMR signals and parameters, such as the phosphorus signals of PKA[9] or the amide signals of selectively labeled cAbl.[21] Clearly, the dynamic nature of protein kinase catalytic domains is one of the most intriguing aspects of this class of enzymes. For a long time, NMR relaxation analysis has been the method of choice to study such processes at atomic resolution. Another aspect of protein kinases, the orientational changes brought about by activation and during the catalytic action of the protein, can be inferred from residual dipolar couplings. Our data are a prerequisite for such investigations.

Another important point of interest is the interaction of protein kinases with small ligands that act as specific inhibitors. Since many protein kinase are causative for different diseases, the finding of new inhibitors showing selective interaction with different protein kinases would be of great pharmaceuti-

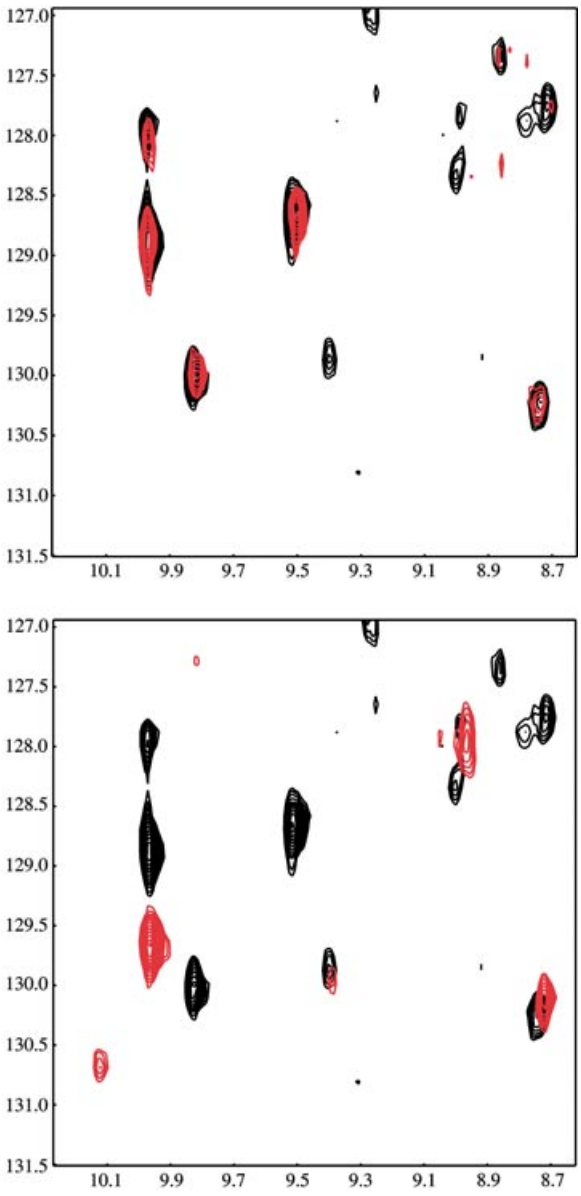

Figure 7. *Comparison of TROSY spectra of wild-type PKA (black) with the non-phosphorylable PKA mutants Thr197Ala (red, top) and PKA Ser338Ala (red, bottom).*

cal value. Here we have demonstrated that the binding region of a standard protein kinase inhibitor can be localized by chemical shift mapping. These mapping data are prerequisites for other sophisticated schemes such as the SAR by NMR protocol[25] or the LIGDOCK procedure[26] and might serve as the basis for the development of new and specific protein kinase inhibitors.

All previously known structures of PKA have been determined with the activated protein kinase, phosphorylated on both Thr197 and Ser338. Both phosphate groups make contacts to other amino acid side chains. These contacts are obviously important for protein stability and also the stability of these phosphate groups. The Ser338Ala mutant displays enzymatic activity comparable to that of the wild-type, whereas the Thr197Ala mutant is enzymatically inactive (Figure 6). Replacement of Ser338 with Ala does not alter the peak pattern of the TROSY spectrum, whereas this is the case for the Thr197Ala mutant. These results suggest that the overall conformation of the Ser338Ala mutant is not altered, but that in the Thr197Ala mutant at least part of the protein undergoes conformational changes. This leads to the assumption that the main function of Ser338 phosphorylation is enhancement of the protein stability. Taken together, our data presented here clearly demonstrate that protein kinases are amenable to NMR study and that NMR should be a very useful tool with which to gain more insight into the structures and dynamics of protein kinases.

Experimental Section

Cloning and expression: A plasmid containing the coding sequence of cAMP-dependent protein kinase catalytic subunit (GPKA) was kindly provided by Dr. Steven Green.[27] This plasmid was used as template. DNA coding for the full-length PKA catalytic subunit was amplified by PCR and cloned into the NdeI/BamHI site of pET16bTev, which is a modified version of the pET16b (Novagen, Madison, WI, USA) expression vector in which the Factor Xa-cleavage site has been replaced by a tobacco etch virus (Tev) protease cleavage site. The resulting expression plasmid pETPKA was used for transformation of *E. coli* strain Bl21 (DE3)/pLysS (Novagen). As a result of cloning and Tev-cleavage, three additional amino acids precede the PKA sequence. Site-specific mutagenesis to replace phosphorylation sites Thr197 and Ser338 with Ala was achieved by the Quick Change protocol (Stratagene). All constructs were verified by sequencing. For uniformly ^{15}N-labeled PKA, cells were grown in M9 minimal-medium containing $^{15}NH_4Cl$ (Eurisotop, Saarbrücken, Germany) as the sole nitrogen source. For production of deuterated and ^{13}C- and ^{15}N-labeled protein, the corresponding IsoGro-medium (Campro Scientific, Berlin) was used, following the manufacturer's recommendations. *E. coli* strain CT19 (kindly provided by Dr. David Waugh, National Cancer Institute, Frederick, MD) was disposed for selective labeling with ^{15}N-containing amino acids. The following labeled amino acids were used: ^{15}N isoleucine, ^{15}N leucine, ^{15}N valine, ^{15}N phenylalanine, ^{15}N aspartate, ^{15}N tyrosine, and 1–^{13}C tyrosine (Eurisotop, Saarbrücken, Germany). The procedure applied for selective amino acid labeling is essentially as described by Muchmore et al.[28] Double selective labeling with 1–^{13}C tyrosine together with ^{15}N valine was carried out accordingly. Cells were grown in the presence of ampicillin (100 $\mu g\,mL^{-1}$) and chloramphenicol (60 $\mu g\,mL^{-1}$) when required at 37 °C until the OD_{600} reached 0.6, and then recombinant protein production was initiated by addition of IPTG (isopropyl β-D-thiogalactopyranoside, 1 mM). Induction was carried out for 18 h at 20 °C, and cells were harvested by centrifugation for 15 min at 4500 *g*. Cell pellets were stored at −80 °C until usage.

Purification of PKA: Cell pellets were thawed and resuspended in NaCl (500 mM), Tris/HCl (pH 8.0, 50 mM), and β-mercaptoethanol (5 mM). Lysozyme (2 mg) and benzonase (Merck, Darmstadt, Germany, 100 U) were added per mL protein suspension. Cells were lyzed by sonification, and the cell debris was removed by centrifugation at 20 000 *g* for 1 hour at 4 °C. The supernatant was applied to a Ni-NTA FastFlow column (Quiagen, Hilden, Germany) following the manufacturer's recommendations. Cleavage of the His-tag was performed with minor modifications as described by Melcher.[29] Further purification was achieved by anion-exchange chromatography with a Source Q column (Pharmacia Biotech). The column was

equilibrated in Hepes (20 mM)/DTT (2 mM, pH 7.2), and bound protein was eluted with a 10 column volume gradient to buffer B (500 mM NaCl, 20 mM Hepes, 2 mM DTT, pH 7.2). Finally, samples were dialyzed against the appropriate buffers (see below). Typical values for the expression yield were 10 mg L^{-1}.

Synthesis of spin-labeled adenosine: 5-Aminoadenosine (BioLog Life Science Institute, Bremen, Germany, 9.96 mg, 36.82 μmol) was added to 1-oxyl-2,2,5,5-tetramethylpyrroline-3-carboxylate *N*-hydroxysuccinimide ester (oxyl-1-NHS, Toronto Research Chemicals Inc., North York, Ontario, Canada, 7.4 mg, 26.3 mmol). The compounds were dissolved in sodium phosphate (20 mM, 150 μL, pH 8.4) and DMSO (650 μL), and the mixture was gently shaken overnight at 4 °C. The solution was then evaporated to dryness in vacuo, and the residue was dissolved in acetonitrile/water (1:1) containing 0.5% TFA (350 μL). Purification of spin-labeled adenosine (1-oxyl-2,2,5,5-tetramethylpyrroline-3-carboxylate (5-aminoadenosine)-amide) was achieved by HPLC on a Eurospher RP-18 column (Knauer, Berlin, Germany). Mass spectroscopic analysis of the desired reaction product gave a value of 433.2 g mol^{-1}, which is in good accordance with the calculated molecular weight of 433.5 g mol^{-1}.

NMR spectroscopy: NMR conditions for triply labeled NMR samples (300 mM NaCl, 5 mM DTT, 50 mM Hepes, pH 6.0, 0.7 mM protein, in 90% H_2O/10% D_2O) were checked by diffusion measurements by use of the bipolar LED pulse sequence on a Bruker DRX 600 spectrometer (Bruker, Karlsruhe, Germany). Both the selectively ^{15}N-labeled samples and the doubly selectively labeled samples were uniformly prepared at 0.25 mM protein concentration with NaCl (100 mM), DTT (5 mM), Hepes (50 mM, pH 6.5) in H_2O/D_2O (90%:10%). 3D triple resonance assignment NMR spectra were acquired at 800 MHz on a four-channel Bruker DRX 800 spectrometer. All experiments were run as TROSY-type experiments[18,19] with deuterium decoupling and residual proton decoupling.[30] For the standard assignment protocol[31] the following backbone assignments were run on triply labeled samples of PKA: 1) HNCO, 2) HN(CA)CO, 3) HNCA, 4) HNCACB, and 5) HN(CO)CACB.

Ligands (spin-labeled adenosine, H7 [Sigma–Aldrich]) were added from stock solutions in [D_6]DMSO (100 mM) to a final concentration of 1 mM. Peak integrals were determined with Bruker xwinnmr software.

Enzymatic assay: The enzymatic activity of PKA proteins was analyzed with the aid of a luminescent kinase assay, following the manufacturer's recommendations (Kinase-Glo, Promega, Madison, WI, USA). Kemptide (Promega) was used as substrate. The enzymatic assay was carried out in Hepes (pH 7.5, 50 mM), NaCl (50 mM), DTT (2 mM), and $MgCl_2$ (10 mM). The optimal ATP and substrate concentrations were estimated as 2.5 and 5 μM, respectively. The amount of PKA proteins employed was 74 nM in all assays. The kinase assays were performed in quadruplicate in 96-well plates, and the luminescence was recorded with a Veritas microplate luminometer (Turner BioSystems, Sunnyvale, CA, USA). Data were analyzed with GraphPad Prism (GraphPad Software, Inc., San Diego, CA, USA).

Assignment: Three-dimensional spectra were evaluated with XEASY.[32] Two-dimensional spectra were analyzed with NMRVIEW[33] by use of in-house tcl scripts. Analysis of structural data and distance measurements was performed with MolMol.[34] Chemical shifts have been deposited in the BioMagRes Bank database under accession number BMRB 6183 (http://www.bmrb.wisc.edu).

Chemical shift matching: Chemical shifts were predicted by use of SHIFTX.[14] Coordinates for pdb entries 1ATP (murine PKA with ATP and inhibitor)[15] and 1J3H (apo-PKA)[16] were used for the prediction. Although the latter structure fits the composition of our NMR sample better, the prediction is biased by missing coordinates in the protein core. In all practical cases, predicted shifts from both structures yield the same results with regard to the location of minima. Chemical shifts were compared with MATLAB by use of in-house scripts. The target function rmsd(A) is defined as:

$$\mathrm{rmsd}(A) = \sqrt{[\sum_{k=A}^{A+L-1} \sum_{i=1}^{S} (\delta_{k,i}^{\mathrm{NMR}} - \delta_{k,i}^{\mathrm{calc}})]^2 / I} \quad (1)$$

Here, rmsd(A) = target function, A = position in sequence, L = length of stretch, S = number of chemical shifts in each residue, δ^{NMR} = experimentally observed chemical shift, δ^{calc} = back-calculated chemical shift.

Acknowledgements

We are grateful to Sarah Mensch, Johann Wolfgang Goethe-Universität, Frankfurt am Main, for HPLC purification of the spin-labeled adenosine derivative.

Keywords: kinase inhibition · NMR spectroscopy · protein kinase A · protein structures · spin-label

[1] G. Manning, D. B. Whyte, R. Martinez, T. Hunter, S. Sudarsanam, *Science* **2002**, *298*, 1912 – 1934.
[2] D. Fabbro, S. Ruetz, E. Buchdunger, S. Cowan-Jacob, G. Fendrich, J. Liebetanz, J. Mestan, T. O'Reilly, P. Traxler, B. Chaudhuri, H. Fretz, J. Zimmermann, T. Meyer, G. Caravatti, P. Furet, P. Manley, *Pharmacol. Therap.* **2002**, *93*, 79 – 98.
[3] M. E. M. Noble, J. A. Endicott, L. N. Johnson, *Science* **2004**, *303*, 1800 – 1805.
[4] D. A. Johnson, P. Akamine, E. Radzio-Andzelm, Madhusudan, S. S. Taylor, *Chem. Rev.* **2001**, *101*, 2243 – 2270.
[5] P. B. Daniel, W. H. Walker, J. F. Habener, *Annu. Rev. Nutr.* **1998**, *18*, 353 – 383.
[6] S. Shoji, K. Titani, J. G. Demaille, E. H. Fischer, *J. Biol. Chem.*, **1979**, *254*, 6211 – 6214.
[7] W. Yonemoto, M. L. McGlone, B. Grant, S. S. Taylor, *Prot. Eng.* **1997**, *10*, 915 – 925.
[8] F. W. Herberg, S. M. Bell, S. S. Taylor, *Prot. Eng.* **1993**, *6*, 771 – 777.
[9] M. H. Seifert, C. B. Breitenlechner, D. Bossemeyer, R. Huber, T. A. Holak, R. A. Engh, *Biochemistry* **2002**, *41*, 5968 – 5977.
[10] J. B. Shabb, *Chem. Rev.* **2001**, *101*, 2381 – 2411.
[11] M. Gaßel, C. B. Breitenlechner, P. Rüger, U. Jucknischke, T. Schneider, R. Huber, D. Bossemeyer, R. A. Engh, *J. Mol. Biol.* **2003**, *329*, 1021 – 1034.
[12] C. Breitenlechner, M. Gaßel, H. Hidaka, V. Kinzel, R. Huber, R. A. Engh, D. Bossemeyer, *Structure* **2003**, *11*, 1595 – 1607.
[13] S. K. Hanks, T. Hunter, *FASEB J.* **1995**, *9*, 576 – 596.
[14] M. Huse, J. Kuriyan, *Cell* **2002**, *109*, 275 – 282.
[15] J. H. Zheng, D. R. Knighton, L. F. Eyck, R. Karlsson, N. H. Xuong, S. S. Taylor, *Biochemistry* **1993**, *32*, 2154 – 2161
[16] P. Akamine, Madhusudan, J. Wu, N. H. Xuong, L. F. Ten Eyck, S. S. Taylor, *J. Mol. Biol.* **2003**, *327*, 159 – 171.
[17] Madhusudan, P. Akamine, N. H. Xuong, S. S. Taylor, *Nat. Struct. Biol.* **2002**, *9*, 273 – 277.
[18] K. Pervushin, R. Riek, G. Wider, K. Wüthrich, *Proc. Natl. Acad. Sci. USA* **1997**, *94*, 12366 – 12371.
[19] M. Salzmann, K. Pervushin, G. Wider, H. Senn, K. Wüthrich, *Proc. Natl. Acad. Sci. USA* **1998**, *95*, 13585 – 13590.

[20] S. Neal, A. M. Nip, H. Zhang, D. S. Wishart, *J. Biomol. NMR* **2003**, *26*, 215 – 240.
[21] A. Strauss, F. Bitsch, B. Cutting, G. Fendrich, P. Graff, J. Liebetanz, M. Zurini, W. Jahnke, *J. Biomol. NMR* **2003**, *26*, 367 – 372.
[22] J. Weigelt, M. van Dongen, J. Uppenberg, J. Schulz, M. Wikström, *J. Am. Chem. Soc. 124*, 2446 – 2447.
[23] R. A. Engh, A. Girod, V. Kinzel, R. Huber, D. Bossemeyer, *J. Biol. Chem.* **1996**, *271*, 26 157 – 26 164
[24] H. Hidaka, M. Inagaki, S. Kawamoto, Y. Sasaki, *Biochemistry* **1984**, *23*, 5036 – 5041.
[25] S. B. Shuker, P. J. Hajduk, R. P. Meadows, S. W. Fesik, *Science* **1996**, *274*, 1531 – 1534.
[26] U. Schieborr, B. Elshorst, M. Vogtherr, M. Betz, S. Grimme, K. Saxena, T. Langer, H. Schwalbe, unpublished results
[27] J. Bok, X.-M. Zha, Y.-S. Cho, S. Green, *J. Neuroscience* **2003**, *23*, 777 – 787.
[28] D. C. Muchmore, L. P. McIntosh, C. B. Russell, D. E. Anderson, F. W. Dahlquist, *Methods Enzymol.* **1989**, *177*, 44 – 73.
[29] K. Melcher, *Anal. Biochem*. **2000**, *277*, 109 – 120.
[30] M. Sattler, J. Schleucher, C. Griesinger, *Prog. NMR Spectr.* **1999**, *34*, 93 – 158.
[31] A. Eletsky, A. Kienhofer, K. Pervushin, *J. Biomol. NMR* **2001**, *20*, 177 – 180.
[32] C. Bartels, T.-H. Xia, M. Billeter, P. Güntert, K. Wüthrich, *J. Biomol. NMR* **1995**, *5*, 1 – 10.
[33] B. A. Johnson, R. A. Blevins, *J. Biomol. NMR* **1994**, *4*, 603 – 614.
[34] R. Konradi, M. Billeter, K. Wüthrich, *J. Mol. Graphics* **1996**, *14*, 51 – 55.

Received: April 30, 2004
Early View Article
Published online on October 13, 2004

